Title

Development of Living Therapeutics via Synthetic Biology

Author

Wu, Yutong

Publication Date

2024

Peer reviewed|Thesis/dissertation

UNIVERSITY OF CALIFORNIA

Los Angeles

Development of Living Therapeutics via Synthetic Biology

A thesis submitted in partial satisfaction

of the requirements for the degree Master of Science

in Chemical Engineering

by

Yutong Wu

2024

ABSTRACT OF THE THESIS

Development of Living Therapeutics via Synthetic Biology

by

Yutong Wu

Master of Science in Chemical Engineering

University of California, Los Angeles, 2024

Professor Philippe Sautet, Chair

Synthetic biology, through a combination of biology, engineering, and computer science, programs cells to perform novel functions. Synthetic cells are engineered to produce biomolecules, act as biosensors, or deliver therapies with precision. As one of the synthetic receptos that are incorporated into the cells, synNotch receptor, derived from Notch receptors, offers precise activation control and is used mainly in cancer therapies. In contrast to the current research focus, our study is centered on developing a therapeutic approach of the regeneration of synNotch via engineering cells with synNotch receptors to create localized immunosuppressive environments for treating Type 1 diabetes. Our design indicates a great potential of protection transplanted beta islets from immune rejection, enhancing the success of islet transplantation for diabetes patients.

This thesis of Yutong Wu is approved.

Song Li

Irene Chen

Philippe Sautet, Committee Chair

University of California, Los Angeles

2024

Table of Contents

List of Figures

Acknowledgements

I would like to express my deepest gratitude to Professor Song Li for his unwavering support and guidance throughout my project and graduate career at UCLA. His invaluable mentorship has provided me with the opportunity to collaborate with a dedicated team in a supportive lab environment. I would also like to express my appreciation to my mentor, Dr. Jana Zarubova, for her invaluable guidance and support throughout this project. Her expertise and encouragement have been crucial in advancing my research and navigating its challenges.

My thanks extend to all the members of the Li Lab for fostering a great working atmosphere and offering their support. Special thanks to former lab members, Dr. Tyler Hoffman, for his technical expertise in cell engineering, and Dr. Mohammad Mahdi Hasani-Sadrabadi, for his suggestions on biomaterials. I am also appreciative of the current lab members: Yifan Wu for her advice on biomaterials, Dr. Parvaiz A. Shiekh for his assistance in making microparticles, Dr. Bo Zhang for his consultation on biomaterials, Dr. Jennifer Soto for her support in cell engineering and as lab manager, and Hye Sook Shin for her guidance on imaging.

Additionally, I am thankful to my committee members, Dr. Philippe Sautet and Dr. Irene Chen, for their support and assistance. Lastly, I acknowledge the funding sources from the Li Lab that have supported this project.

Chapter 1: Introduction

Synthetic biology, an interdisciplinary field which combines biology, engineering, and computer science, is revolutionizing how we approach biological systems by allowing us to program cells to perform novel and complex functions[1].This innovative field holds promise in various domains, including medicine, agriculture, environmental management, and industrial biotechnology[2,3]. One of the most powerful tools developed through synthetic biology is synthetic cells, which offer numerous advantages over natural cells. These engineered cells can be customized to perform specific tasks, such as producing complex biomolecules or synthesizing drugs that are difficult to obtain through conventional methods[4]. Additionally, synthetic cells can be designed with built-in safety mechanisms, such as self-destruction capabilities, to limit their replication and reduce the risk of unintended consequences[5]. This is particularly important in applications where long-lasting effects of engineered cells could pose a threat. Furthermore, synthetic cells can function as highly sensitive biosensors, capable of detecting specific molecules in the environment[6]. Another critical application of synthetic cells is in targeted drug delivery, where they can deliver therapeutic agents with high precision to specific tissues or cells, thereby enhancing the efficacy of treatments while minimizing side effects[7]. To achieve such precise targeting, synthetic receptors like Chimeric Antigen Receptors (CARs) and synthetic Notch (synNotch) receptors have been developed. CARs are programmed to recognize specific antigens on tumor cells, such as CD19, and initiate precise killing of these cells as part of cancer treatment[8-10]. SynNotch receptors, derived from the Notch family of transmembrane proteins involved in cell-cell communication, offer even greater flexibility and precision[11-14]. Notch receptors play a crucial role in processes like angiogenesis, where they regulate the formation and branching of new blood vessels[15]. By modifying Notch receptors, scientists have created synNotch receptors, which allow for the definition of both novel inputs and outputs in engineered cells[11]. Unlike CARs, synNotch receptors require mechanical force, such as binding to a surface or a bead, for activation, making them highly selective[16-18]. This property has made synNotch receptors particularly

valuable in cancer therapies, where they can complement CAR technology to reduce off-target effects and improve treatment specificity[12,13].

While the major applications of synNotch technology have been demonstrated in cancer treatment, its application in regenerative medicine remains unexplored. To address this gap, our research focuses on using these synthetic receptors to develop living immunotherapeutics for treating Type 1 diabetes, a chronic autoimmune disease characterized by the destruction of pancreatic beta cells by the immune system[19]. Type 1 diabetes primarily affects the pediatric population in the U.S., accounting for over 85% of diabetes cases among young people[20]. While insulin injections are the standard treatment, beta islet transplantation offers a more permanent solution for severe cases[21,22]. However, the major challenge with beta islet transplantation is immune rejection, as the overactive immune system in Type 1 diabetes patients continuously attacks the newly transplanted beta islets[21]. Traditional approaches, such as encapsulating islets in alginate hydrogels, provide some protection by creating a physical barrier against immune cells, but they have limitations[23,24]. The hydrogel barrier may not completely prevent immune cells and antibodies from reaching the islets, and diffusion limitations can lead to hypoxia and nutrient depletion[25].

To overcome these challenges, we develop a novel approach by engineering synthetic cells with synNotch receptors which can be transplanted with beta islets. These synthetic cells are designed to create a localized immunosuppressive environment to protect the transplanted beta islets from immune attacks. The synNotch circuit we have developed is activated when the synthetic cells come into contact with a biomaterial-bound ligand (e.g., mCherry), triggering the release of a potent transcription factor which drives the expression of two immunosuppressive molecules, Interleukin-10 (IL-10) and Programmed Death-Ligand 1 (PD-L1)[32]. IL-10 is a cytokine with strong anti-inflammatory and immunosuppressive properties, but it faces challenges in stability and potential toxicity when administered systemically[26,27]. By engineering synthetic cells to produce IL-10 locally, we aim to achieve prolonged immunosuppression at the site of transplantation without the adverse effects associated with systemic delivery[28]. PD-L1, on

the other hand, plays a crucial role in inducing immune tolerance by binding to PD-1 on immune cells, reducing their proliferation and cytokine production[29,30]. Together, the local release of IL-10 and the expression of PD-L1 by our engineered synthetic cells create a protective niche for the transplanted beta islets, enhancing their survival and function in Type 1 diabetes patients. This dual-function approach, leveraging the precision and modularity of synNotch receptors, represents a promising new direction in the treatment of autoimmune diseases through synthetic biology.

In our study, we first generated the synthetic cells to secrete the IL-10 and express PD-L1 in response to synNotch activation. To trigger this activation, we bound mCherry to a surface—either hydrogel or microparticles—and conducted characterization of the material to ensure that the mCherry was successfully anchored to the surface. After confirming the surface-bound mCherry, we demonstrated that the synthetic cells were effectively activated upon contact with the mCherry attached to these materials. Once activated, the synthetic cells produced a conditioned medium containing IL-10, which we collected for further analysis. To evaluate the immunosuppressive potential of this conditioned medium, we co-incubated it with primary $CD4^+$ T cells isolated from the mouse. Our results revealed a marked increase in the formation of regulatory T cells (Tregs), a critical subset involved in immune tolerance[31]. This increase in Treg cell population suggests that the conditioned medium, produced by the activated synthetic cells, promotes the development of an immunosuppressive microenvironment in vitro. These findings highlight the promise of this approach in preventing immune-mediated rejection of transplanted beta islets. By co-injecting synthetic cells with beta islets, this strategy fosters a localized immunosuppressive environment through the sustained release of IL-10 and the expression of PD-L1 on synthetic cells. This approach could protect transplanted islets from immune attack to enhance the long-term success of islet transplantation as a therapeutic option for patients with Type 1 diabetes. Overall, our work highlights the potential of cells incoporated with synNotch receptors as an immunotherapeutic tool in both regenerative medicine and the treatment of diabetes.

References

1. Tan, X., Letendre, J. H., Collins, J. J., & Wong, W. W. (2021). Synthetic biology in the clinic: engineering vaccines, diagnostics, and therapeutics. *Cell*, *184*(4), 881-898.
2. Smolke, C. D., & Silver, P. A. (2011). Informing biological design by integration of systems and synthetic biology. *Cell*, *144*(6), 855-859.
3. Clarke, L., & Kitney, R. (2020). Developing synthetic biology for industrial biotechnology applications. *Biochemical Society Transactions*, *48*(1), 113-122.
4. Guindani, C., da Silva, L. C., Cao, S., Ivanov, T., & Landfester, K. (2022). Synthetic cells: from simple bio-inspired modules to sophisticated integrated systems. *Angewandte Chemie*, *134*(16), e202110855.
5. Pasotti, L., Zucca, S., Lupotto, M., Cusella De Angelis, M. G., & Magni, P. (2011). Characterization of a synthetic bacterial self-destruction device for programmed cell death and for recombinant proteins release. *Journal of biological engineering*, *5*, 1-12.
6. Boyd, M. A., & Kamat, N. P. (2021). Designing artificial cells towards a new generation of biosensors. *Trends in biotechnology*, *39*(9), 927-939.
7. Ghosh, B. (2022). Artificial cell design: reconstructing biology for life science applications. *Emerging Topics in Life Sciences*, *6*(6), 619-627.
8. Davila, M. L., & Brentjens, R. J. (2016). CD19-Targeted CAR T cells as novel cancer immunotherapy for relapsed or refractory B-cell acute lymphoblastic leukemia. *Clinical advances in hematology & oncology: H&O*, *14*(10), 802.
9. Park, J. H., Geyer, M. B., & Brentjens, R. J. (2016). CD19-targeted CAR T-cell therapeutics for hematologic malignancies: interpreting clinical outcomes to date. *Blood, The Journal of the American Society of Hematology*, *127*(26), 3312-3320.
10. Labanieh, L., Majzner, R. G., & Mackall, C. L. (2018). Programming CAR-T cells to kill cancer. *Nature biomedical engineering*, *2*(6), 377-391.

11. Morsut, L., Roybal, K. T., Xiong, X., Gordley, R. M., Coyle, S. M., Thomson, M., & Lim, W. A. (2016). Engineering customized cell sensing and response behaviors using synthetic notch receptors. *Cell*, *164*(4), 780-791.
12. Roybal, K. T., Rupp, L. J., Morsut, L., Walker, W. J., McNally, K. A., Park, J. S., & Lim, W. A. (2016). Precision tumor recognition by T cells with combinatorial antigen-sensing circuits. *Cell*, *164*(4), 770-779.
13. Choe, J. H., Watchmaker, P. B., Simic, M. S., Gilbert, R. D., Li, A. W., Krasnow, N. A., ... & Lim, W. A. (2021). SynNotch-CAR T cells overcome challenges of specificity, heterogeneity, and persistence in treating glioblastoma. *Science translational medicine*, *13*(591), eabe7378.
14. Ruffo, E., Butchy, A. A., Tivon, Y., So, V., Kvorjak, M., Parikh, A., ... & Lohmueller, J. (2023). Post-translational covalent assembly of CAR and synNotch receptors for programmable antigen targeting. *Nature Communications*, *14*(1), 2463.
15. Akil, A., Gutiérrez-García, A. K., Guenter, R., Rose, J. B., Beck, A. W., Chen, H., & Ren, B. (2021). Notch signaling in vascular endothelial cells, angiogenesis, and tumor progression: an update and prospective. *Frontiers in cell and developmental biology*, *9*, 642352.
16. He, L., & Perrimon, N. (2023). Synthetic Notch receptors and their applications to study cell-cell contacts in vivo. *Developmental Cell*, *58*(3), 171-173.
17. Sloas, D. C., Tran, J. C., Marzilli, A. M., & Ngo, J. T. (2023). Tension-tuned receptors for synthetic mechanotransduction and intercellular force detection. *Nature biotechnology*, *41*(9), 1287-1295.
18. Garibyan, M., Hoffman, T., Makaske, T., Do, S. K., Wu, Y., Williams, B. A., ... & Morsut, L. (2024). Engineering programmable material-to-cell pathways via synthetic notch receptors to spatially control differentiation in multicellular constructs. *Nature Communications*, *15*(1), 5891.
19. Bresson, D., & von Herrath, M. (2004). Mechanisms underlying type 1 diabetes. *Drug Discovery Today: Disease Mechanisms*, *1*(3), 321-327.

20. Imperatore, G., Mayer-Davis, E. J., Orchard, T. J., & Zhong, V. W. (2021). Prevalence and incidence of type 1 diabetes among children and adults in the United States and comparison with non-US countries.
21. Kabakchieva, P., Assyov, Y., Gerasoudis, S., Vasilev, G., Peshevska-Sekulovska, M., Sekulovski, M., ... & Velikova, T. (2023). Islet transplantation-immunological challenges and current perspectives. *World Journal of Transplantation*, *13*(4), 107.
22. Bruni, A., Gala-Lopez, B., Pepper, A. R., Abualhassan, N. S., & Shapiro, A. J. (2014). Islet cell transplantation for the treatment of type 1 diabetes: recent advances and future challenges. *Diabetes, metabolic syndrome and obesity: targets and therapy*, 211-223.
23. Zhang, Q., Gonelle-Gispert, C., Li, Y., Geng, Z., Gerber-Lemaire, S., Wang, Y., & Buhler, L. (2022). Islet encapsulation: new developments for the treatment of type 1 diabetes. *Frontiers in Immunology*, *13*, 869984.
24. Ghasemi, A., Akbari, E., & Imani, R. (2021). An overview of engineered hydrogel-based biomaterials for improved β-cell survival and insulin secretion. *Frontiers in Bioengineering and Biotechnology*, *9*, 662084.
25. Espona-Noguera, A., Ciriza, J., Cañibano-Hernández, A., Orive, G., Hernández, R. M., Saenz del Burgo, L., & Pedraz, J. L. (2019). Review of advanced hydrogel-based cell encapsulation systems for insulin delivery in type 1 diabetes mellitus. *Pharmaceutics*, *11*(11), 597.
26. Iyer, S. S., & Cheng, G. (2012). Role of interleukin 10 transcriptional regulation in inflammation and autoimmune disease. *Critical Reviews™ in Immunology*, *32*(1).
27. Carlini, V., Noonan, D. M., Abdalalem, E., Goletti, D., Sansone, C., Calabrone, L., & Albini, A. (2023). The multifaceted nature of IL-10: regulation, role in immunological homeostasis and its relevance to cancer, COVID-19 and post-COVID conditions. *Frontiers in immunology*, *14*, 1161067.

28. Abbaszadeh, S., Nosrati-Siahmazgi, V., Musaie, K., Rezaei, S., Qahremani, M., Xiao, B., ... & Shahbazi, M. A. (2023). Emerging strategies to bypass transplant rejection via biomaterial-assisted immunoengineering: Insights from islets and beyond. *Advanced Drug Delivery Reviews*, 115050.
29. Gutic, B., Bozanovic, T., Mandic, A., Dugalic, S., Todorovic, J., Stanisavljevic, D., ... & Soares, J. M. (2023). Programmed cell death-1 and its ligands: current knowledge and possibilities in immunotherapy. *Clinics*, *78*, 100177.
30. Parvez, A., Choudhary, F., Mudgal, P., Khan, R., Qureshi, K. A., Farooqi, H., & Aspatwar, A. (2023). PD-1 and PD-L1: architects of immune symphony and immunotherapy breakthroughs in cancer treatment. *Frontiers in Immunology*, *14*, 1296341.
31. Goswami, T. K., Singh, M., Dhawan, M., Mitra, S., Emran, T. B., Rabaan, A. A., ... & Dhama, K. (2022). Regulatory T cells (Tregs) and their therapeutic potential against autoimmune disorders–Advances and challenges. *Human vaccines & immunotherapeutics*, *18*(1), 2035117.

Chapter 2: Construction of synthetic cells

2.1 Introduction

Immunoengineering is an interdisciplinary field that combines principles of immunology and bioengineering to manipulate and modulate the immune system for therapeutic purposes. This approach aims to develop novel therapies that can either enhance or suppress immune responses, depending on the clinical need[1]. Current immunological strategies include the design of immune-modulating biomaterials, cellular therapies, and synthetic biological systems like the synNotch circuit, which can precisely control immune cell behavior in a targeted manner[2,3]. Immunotherapies such as checkpoint inhibitors, CAR-T cell therapy, and regulatory T cell (Treg) modulation are examples of immunological approaches that are transforming treatments for cancer, autoimmune diseases, and organ transplantation[4]. Nonetheless, the application of the synNotch receptor in the field of regeneration remains largely unexplored. To investigate its potential in this field, synthetic cells were engineered to secrete IL-10 and express PD-L1 upon synNotch activation. These modifications are designed to create an immunosuppressive environment, facilitating tissue regeneration by promoting immune tolerance and protecting transplanted cells from immune rejection.

2.2 Results and Discussion

2.2.1 Construction of synNotch fibroblasts and T cell

To design and customize a synthetic circuit aimed at treating autoimmune diseases and aiding with the development of regenerative medicine, we utilized mCherry as a model activation signal. During the activation process, the activation signal was bound to a surface to interact with mCherry nanobody binding receptors, which were engineered to be expressed on the surface of synthetic cells. Upon mCherry binding, the receptor triggered the cleavage of the Gal4-VP64 fusion protein. Gal4, a yeast-

derived DNA-binding domain, then localized to upstream activating sequences (UAS) within the plasmid, allowing the VP64 transcriptional activation domain to initiate robust transcription of downstream genes[34]. In our design, this induces the production of IL-10 and PD-L1, leading to IL-10 secretion and PD-L1 surface expression on the synthetic cells, both of which contribute to the creation of a localized immunosuppressive environment **(Figure 2.1)**.

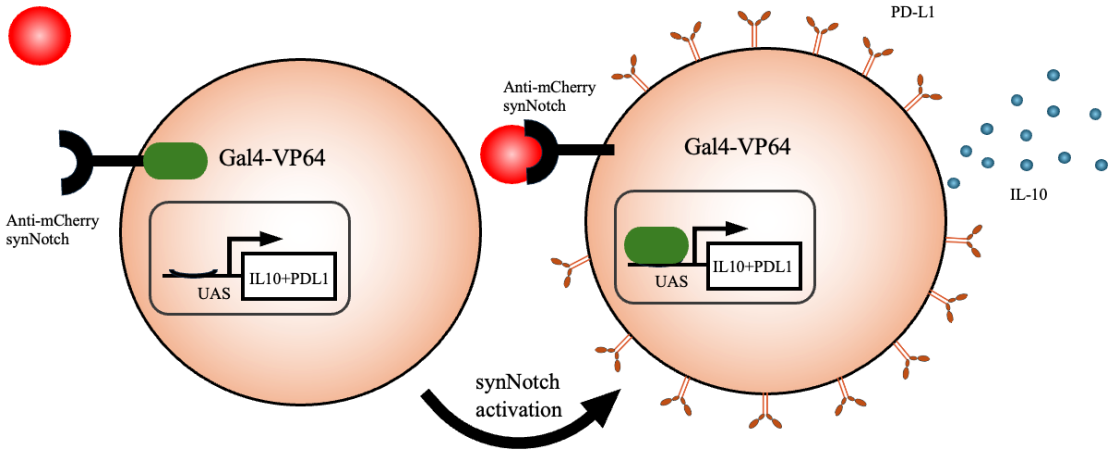

Figure 2. 1: Schematic representation of the synthetic cell activation system. mCherry was used as the model activation signal. During the activation process, surface-immobilized mCherry binds to mCherry-specific nanobody receptors expressed on synthetic cells. Upon binding, the receptor triggers the cleavage of the Gal4-VP64 fusion protein. The yeast-derived Gal4 DNA-binding domain then targets upstream activating sequences (UAS) in the plasmid, enabling the VP64 transcriptional activation domain to drive the expression of downstream genes. In our design, this results in the expression of IL-10 and PD-L1, leading to IL-10 secretion and PD-L1 surface expression for the synthetic cells.

To implant this synthetic circuit into the cells, we first transfected competent E. coli cells with the plasmid using heat shock, selecting for those carrying the plasmid by growing the bacteria on agar plates containing ampicillin. Positive colonies were expanded in liquid culture, and plasmid DNA was isolated for further use. The plasmid was then transfected into HEK 293T cells along with lentiviral packaging vectors, enabling the production of viral particles containing the plasmid. These viral particles were used

to transduce NIH/3T3 fibroblast and Jurkat cells, allowing the plasmid to be introduced into these cell types. After transduction with lentivirus, the cells were sorted **(Figure 2.2)**. Fibroblasts were transduced and sorted because they can be co-injected subcutaneously with the biomaterial to establish a localized immunosuppressive environment. Jurkat cells were chosen due to their ability to circulate systemically and become activated locally at sites where the activation signal is present.

For the fibroblasts, parental cells were co-transduced with the synNotch receptor and the transgene receptor, and the double-positive population which contains both synNotch reporter and transgene receptor was sorted. As illustrated in the figure, this double-positive population accounted for 22.8% of the parental cells. In contrast, Jurkat cells were first transduced with the synNotch receptor, and the positive population was sorted. These sorted cells (synNotch^{+} population) were then transduced with the transgene receptor, and the double-positive population which contains both synNotch reporter and transgene receptor was sorted again, representing 33.9% of the parent population, as shown in the figure. This sequential transduction process was implemented to maximize the percentage of the double-positive population of the parental cells, given the greater difficulty in transducing Jurkat cells compared to fibroblasts.

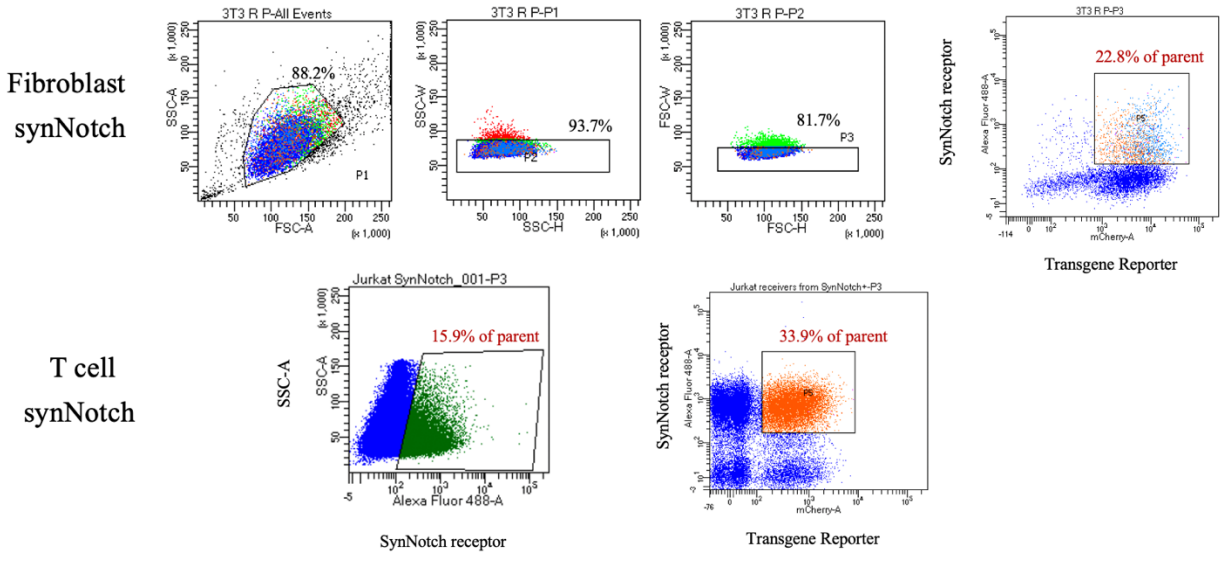

Figure 2. 2: Sorting of synNotch fibroblasts and T cells after lentiviral transduction. NIH/3T3 fibroblasts and Jurkat cells were transduced with lentivirus and sorted afterwards. Fibroblasts were transduced and sorted due to

their ability to be co-injected subcutaneously with biomaterial, establishing a localized immunosuppressive environment. Jurkat cells were selected for their capacity to circulate systemically and be activated locally where the activation signal is present. For fibroblasts, parental cells were co-transduced with synNotch and transgene receptors, and the sorted double-positive population, containing both synNotch reporter and transgene receptor, accounted for 22.8% of the total. For Jurkat cells, sequential transduction was employed to optimize double-positive sorting. Cells were first transduced with the synNotch receptor, followed by sorting of the $SynNotch^{+}$ population. These cells were then transduced with the transgene receptor, and the sorted double-positive population accounted for 33.9% of the total. This process was designed to maximize the percentage of double-positive cells, as Jurkat cells are more challenging to transduce than fibroblasts.

Through this approach, we successfully demonstrated the implantation of the SynNotch circuit into synthetic cells. We also showed that the synNotch circuit can be integrated not only into fibroblasts but also T cells, with the potential for integration of synNotch circuit in other cell types. These results provide a strong foundation for further characterization, evaluation, and development in our following research experiments.

3.2 SynNotch activation by plate bound mCherry

To evaluate the activation of the integrated synNotch receptors, the synNotch fibroblasts and T cells were tested for synNotch activation by the plate bound mCherry protein. mCherry protein was applied to the well plate at a density of 10 μg/cm². Protected from the light, the plate was then left to dry overnight in a biosafety cabinet, then rinsed once with PBS before cell seeding. Anti-mCherry synNotch fibroblasts were seeded at a density of 5×10^4 cells/cm² and cultured for 72 hours for synNotch activation **(Figure 2.3)**. In contrast, anti-mCherry synNotch fibroblasts were seeded at a density of 100,000 cells/well in a 96 well plate and cultured for 72 hours for synNotch activation **(Figure 2.4)**. Afterward, the conditioned medium and cells were collected for subsequent analysis of ELISA and flow cytometry, respectively.

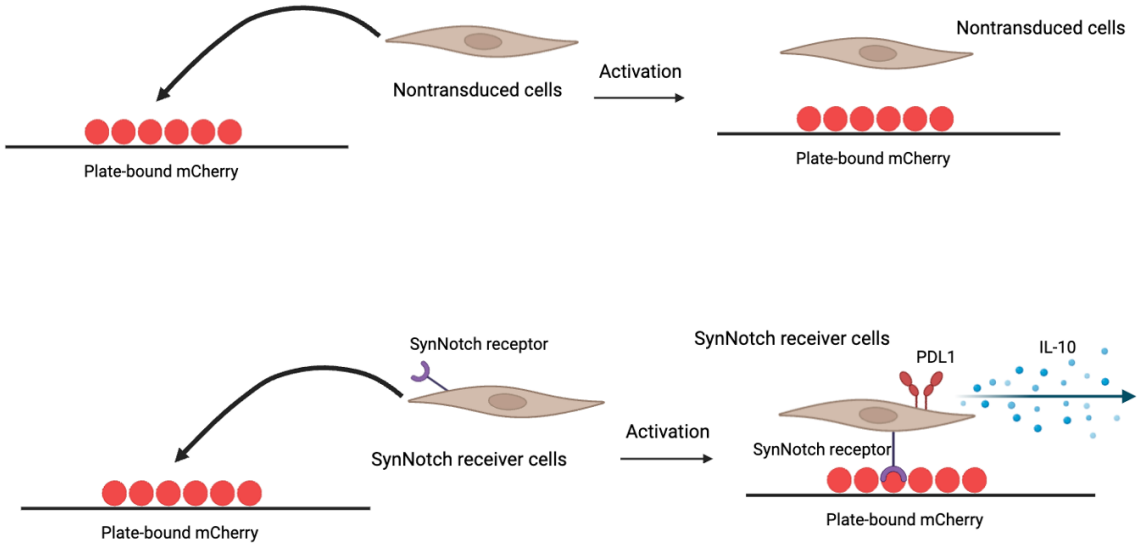

Figure 2. 3: Schematic representation of the synthetic fibroblast activation via plate bound mCherry. mCherry protein was added to the well plate at a density of 10 µg/cm². The plate was then left to dry overnight in a biosafety cabinet protected from the light, then rinsed once with PBS before cell seeding. Anti-mCherry synNotch fibroblasts were seeded at a density of 5×10^4 cells/cm² and cultured for 72 hours. Following the incubation, the conditioned medium and cells were collected for subsequent analysis by ELISA and flow cytometry, respectively, for synNotch activation.

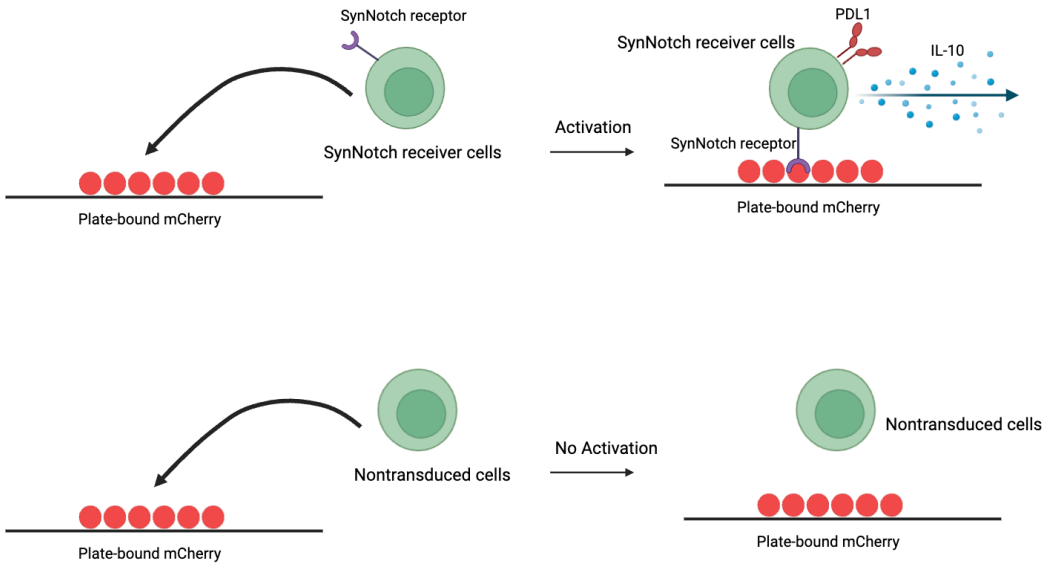

Figure 2. 4: Schematic representation of the synthetic T cell activation via plate bound mCherry. mCherry protein was added to the well plate at a density of 10 µg/cm². The plate was then left to dry overnight in a biosafety cabinet protected from the light, then rinsed once with PBS before cell seeding. Anti-mCherry synNotch T cells were seeded at a density of 100,000 cells/well in a 96 well plate and cultured for 72 hours. After incubation, the conditioned medium and cells were collected for subsequent analysis by ELISA and flow cytometry, respectively, for synNotch activation.

To illustrate the effect of activating the integrated synNotch receptors via plate bound mCherry, ELISA was performed to quantify IL-10 secretion after synNotch activation. The concentration of IL-10 was measured in the conditioned medium collected 72 hours after cell seeding for synNotch activation through ELISA. The results for synNotch fibroblast activation are shown in the figure, where the parental fibroblasts exhibit minimal IL-10 secretion, around 0 pg/mL, regardless of whether they are seeded with or without the activation signal (i.e., plate-bound mCherry). In contrast, synNotch fibroblasts secrete approximately 5,000 pg/mL of IL-10 in the absence of the activation signal. However, when synNotch fibroblasts are seeded with the activation signal, IL-10 secretion increases significantly to approximately 25,000 pg/mL **(Figure 2.5)**.

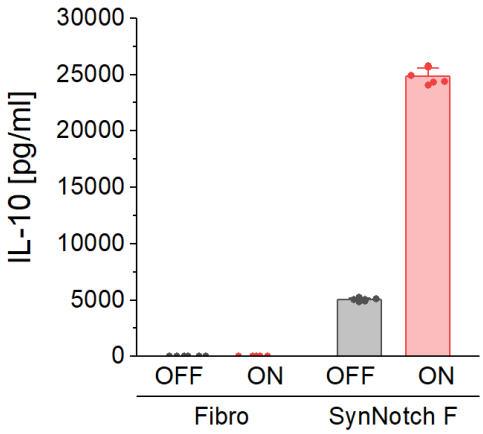

Figure 2. 5: IL-10 secretion by synNotch fibroblasts upon synNotch activation via plate bound mCherry. ELISA was conducted to measure the concentration of IL-10 by synNotch fibroblasts following synNotch activation. IL-10 levels were quantified in the conditioned medium collected 72 hours after cell seeding for synNotch activation by plate bound mCherry. Parental fibroblasts secrete negligible amounts of IL-10 (approximately 0 pg/mL), regardless of the presence or absence of the activation signal (i.e., plate-bound mCherry). In contrast, synNotch fibroblasts secrete about 5,000 pg/mL of IL-10 in the absence of the activation signal. When these fibroblasts are seeded with the activation signal, IL-10 secretion increases markedly to approximately 25,000 pg/mL.

In addition, the results for SynNotch T cell activation are shown. Parental Jurkat cells exhibit minimal IL-10 secretion, around 0 pg/mL, regardless of whether they are seeded with or without the activation signal (i.e., plate-bound mCherry). Besides, SynNotch T cells also secrete approximately 0 pg/mL of IL-10 in the absence of the activation signal. However, when SynNotch T cells are seeded with the activation signal, IL-10 secretion increases significantly to approximately 1,300 pg/mL **(Figure 3.6)**.

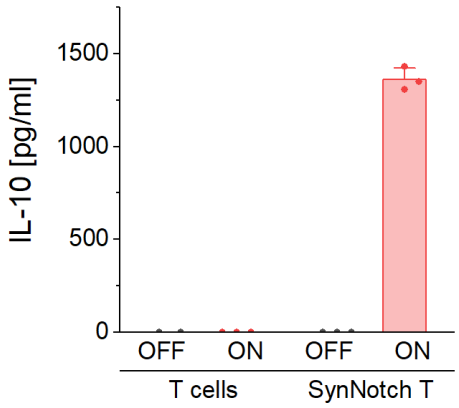

Figure 2. 6: IL-10 secretion by synNotch T cells upon synNotch activation via plate bound mCherry. ELISA was conducted to measure the concentration of IL-10 by synNotch T cells following synNotch activation. IL-10 levels were quantified in the conditioned medium collected 72 hours after cell seeding for synNotch activation by plate bound mCherry. Parental Jurkat cells secrete negligible amounts of IL-10 (approximately 0 pg/mL), regardless of the presence or absence of the activation signal (i.e., plate-bound mCherry). Besides, synNotch T cells also secrete approximately 0 pg/mL of IL-10 in the absence of the activation signal. When these T cells are seeded with the activation signal, IL-10 secretion increases markedly to approximately 1,300 pg/mL.

Note that T cells generally exhibit lower IL-10 secretion compared to fibroblasts. This difference is likely due to the smaller size of T cells and the challenges associated with transducing them compared to fibroblasts. Overall, the results demonstrate the successful integration and activation of the synNotch circuit in both fibroblasts and T cells with plate bound mCherry. Since IL-10 secretion serves as a key criterion for evaluating synNotch activation, the increased IL-10 secretion in the conditioned medium after synNotch activation confirms effective integration of the synNotch receptor and activation of the synNotch receptor by plate bound mCherry.

To further illustrate the effect of activating the integrated synNotch receptors via plate bound mCherry, flow cytometry analysis was performed for the cells harvested after synNotch activation. synNotch fibroblasts and T cells were stained for synNotch receptor, consitutive transgene receptor marker, and the induciable expression of PD-L1 72 hours after cell seeding for synNotch activation. A representive dot plot for flow cytometry for synNotch activation is shown for synNotch fibroblast **(Figure**

2.7). In this figure, parental fibroblasts show minimal PD-L1 expression, with approximately 0% of cells co-expressing both PD-L1 and the constitutive transgene receptor marker, regardless of exposure to the activation signal (i.e., plate-bound mCherry). Similarly, synNotch fibroblasts exhibit around 6.5% co-expression of PD-L1 and the constitutive transgene receptor in the absence of the activation signal. However, when synNotch fibroblasts are exposed to the activation signal, the double-positive population for PD-L1 and the constitutive transgene receptor increases significantly to 85.9%.

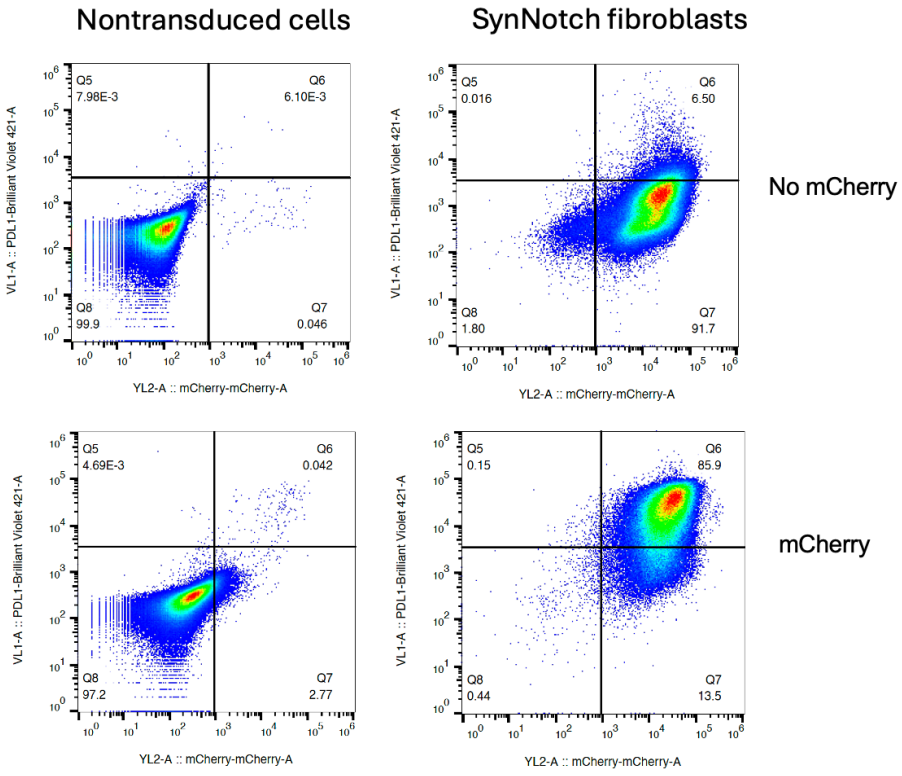

Figure 2. 7: Representive dot plot for flow cytometry for synNotch fibroblast upon synNotch activation via plate bound mCherry. Flow cytometry analysis was conducted on cells collected 72 hours after seeding for synNotch activation. SynNotch fibroblasts were stained for expression of synNotch receptors, the expression of constitutive transgene receptors, and the inducible expression of PD-L1. Parental fibroblasts exhibit negligible PD-L1 expression, with approximately 0% of cells co-expressing both PD-L1 and the constitutive transgene receptor, regardless of the presence or absence of the activation signal (i.e., plate-bound mCherry). Similarly, synNotch fibroblasts show around 6.5% co-expression of PD-L1 and the constitutive transgene receptor in the absence of the

activation signal. However, when these synNotch fibroblasts are exposed to the activation signal, the PD-L1 and constitutive transgene receptor double positive population increases markedly to 85.9%.

For flow cytometry analysis of synNotch fibroblast upon synNotch activation, the percentage of PD-L1$^+$ cells and the median fluorscence intensity (MFI) of PD-L1$^+$ cells are quantified **(Figure 2.8)**. In terms of the percentage of PD-L1$^+$ cells **(Figure 2.8, left)**, parental fibroblasts show minimal PD-L1 expression, with approximately 0% of cells co-expressing both PD-L1 and the constitutive transgene receptor marker, regardless of exposure to the activation signal (i.e., plate-bound mCherry). Similarly, synNotch fibroblasts exhibit around 5% co-expression of PD-L1 and the constitutive transgene receptor in the absence of the activation signal. However, when synNotch fibroblasts are exposed to the activation signal, the double-positive population for PD-L1 and the constitutive transgene receptor increases significantly to 75%. With resepct to the MFI of PD-L1$^+$ cells **(Figure 2.8, right)**, similar trend is observed. Parental fibroblasts exhibit minimal PD-L1 expression, with MFI values around 86 and 270 for cells exposed or not exposed to the activation signal (i.e., plate-bound mCherry), respectively. Besides, synNotch fibroblasts show an MFI value of approximately 1,000 for PD-L1 expression in the absence of the activation signal. However, when synNotch fibroblasts are exposed to the activation signal, the MFI for PD-L1 expression in the positive population increases significantly to around 18,000.

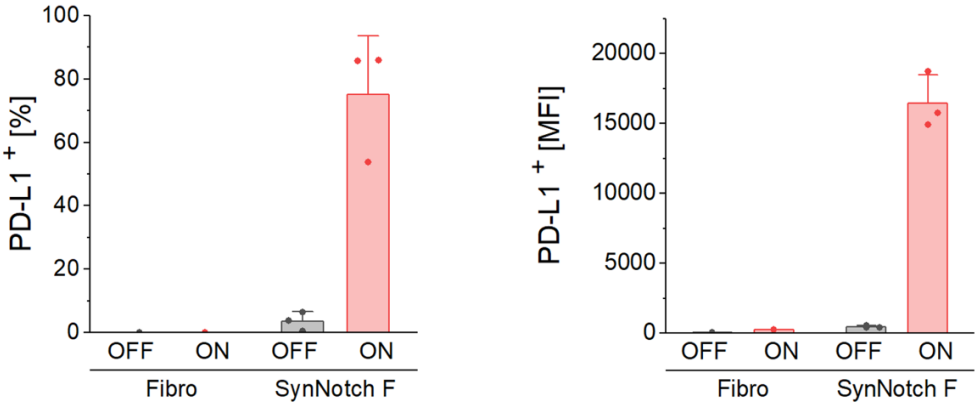

Figure 2. 8: Quantification of PD-L1 expression in synNotch fibroblasts by flow cytometry through percentage of PD-L1$^+$ cells and Median Fluorescence Intensity (MFI) following synNotch activation via plate

bound mCherry. Flow cytometry analysis was conducted on cells collected 72 hours after seeding for synNotch activation. SynNotch fibroblasts were stained for expression of synNotch receptors, the expression of constitutive transgene receptors, and the inducible expression of PD-L1. The left panel shows results for the percentage of PD-L1$^+$ cells upon synNotch activation. Parental fibroblasts display minimal PD-L1 expression, with approximately 0% of cells co-expressing both PD-L1 and the constitutive transgene receptor marker, regardless of whether they are exposed to the activation signal of plate-bound mCherry. In contrast, synNotch fibroblasts show around 5% co-expression of PD-L1 and the constitutive transgene receptor in the absence of the activation signal. However, upon exposure to the activation signal, the percentage of double-positive cells for PD-L1 and the constitutive transgene receptor rises significantly to 75%. The results for median fluorescence intensity (MFI) of PD-L1$^+$ cells shows a comparable trend in the right panel. Parental fibroblasts exhibit minimal PD-L1 expression, with MFI values around 86 and 270 for cells with or without the activation signal, respectively. In contrast, synNotch fibroblasts display an MFI value of approximately 1,000 for PD-L1 expression in the absence of the activation signal. When exposed to the activation signal, the MFI for PD-L1 expression in synNotch fibroblasts increases dramatically to around 18,000.

In addition, the results for synNotch T cell activation are shown **(Figure 2.9)**. In this figure, parental Jurkat cells display minimal PD-L1 expression, with approximately 0% of cells co-expressing both PD-L1 and the constitutive transgene receptor, regardless of activation signal exposure (i.e., plate-bound mCherry). Similarly, synNotch T cells show around 0% co-expression of PD-L1 and the constitutive transgene receptor in the absence of the activation signal. However, when synNotch T cells are exposed to the activation signal, the population of cells co-expressing PD-L1 and the constitutive transgene receptor rises significantly to 32.7%.

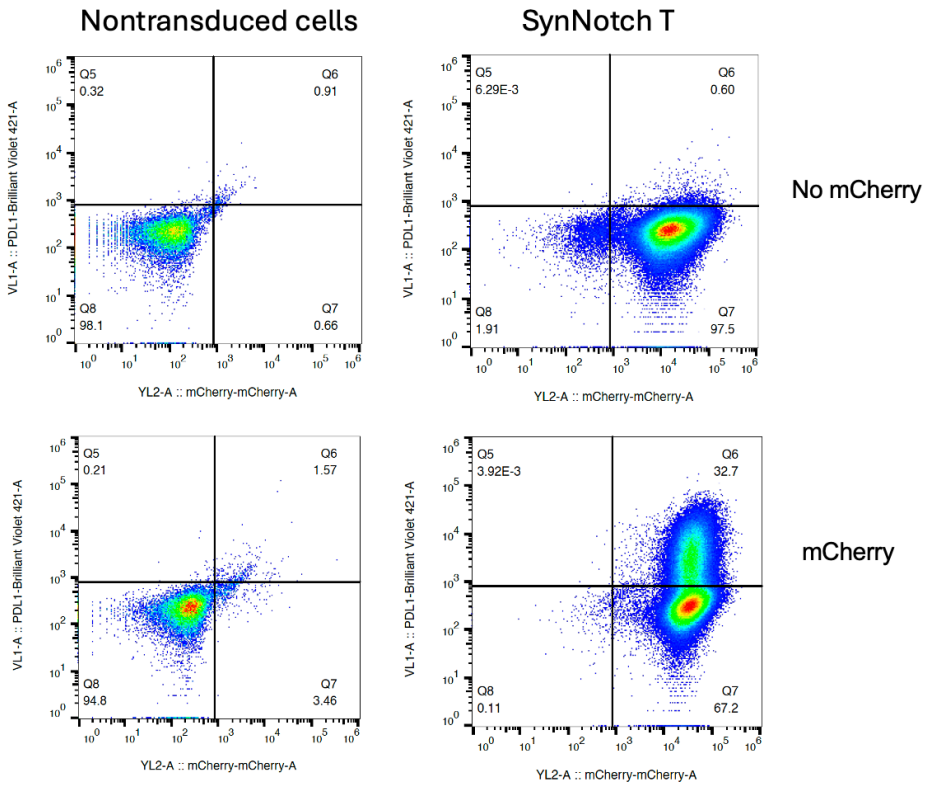

Figure 2. 9: Representive dot plot for flow cytometry for synNotch T cell upon synNotch activation via plate bound mCherry. Flow cytometry analysis was conducted on cells collected 72 hours after seeding for synNotch activation. SynNotch T cells were stained for expression of synNotch receptors, the expression of constitutive transgene receptors, and the inducible expression of PD-L1. Parental Jurkat cells exhibit negligible PD-L1 expression, with approximately 0% of cells co-expressing both PD-L1 and the constitutive transgene receptor, regardless of the presence or absence of the activation signal (i.e., plate-bound mCherry). Similarly, synNotch T cells show around 0% co-expression of PD-L1 and the constitutive transgene receptor in the absence of the activation signal. However, when these synNotch T cells are exposed to the activation signal, the PD-L1 and constitutive transgene receptor double positive population increases significantly to 32.7%.

For flow cytometry analysis of synNotch T cells upon synNotch activation, the percentage of PD-L1$^+$ cells and the median fluorscence intensity (MFI) of PD-L1$^+$ cells are quantified **(Figure 2.10)**. In terms of the percentage of PD-L1$^+$ cells **(Figure 2.10, left)**, parental Jurkat cells show minimal PD-L1 expression, with approximately 0% of cells co-expressing both PD-L1 and the constitutive transgene

receptor marker, regardless of exposure to the activation signal (i.e., plate-bound mCherry). Similarly, synNotch T cells exhibit around 0% co-expression of PD-L1 and the constitutive transgene receptor in the absence of the activation signal. However, when synNotch T cells are exposed to the activation signal, the double-positive population for PD-L1 and the constitutive transgene receptor increases significantly to around 32%. With resepct to the MFI of PD-L1$^+$ cells **(Figure 2.10, right)**, similar trend is observed. Parental Jurkat cells exhibit minimal PD-L1 expression, with MFI values around 200 for cells exposed or not exposed to the activation signal (i.e., plate-bound mCherry). Besides, synNotch fibroblasts show an MFI value of approximately 200 for PD-L1 expression in the absence of the activation signal. However, when synNotch T cells are exposed to the activation signal, the MFI for PD-L1 expression in the positive population increases significantly to around 450.

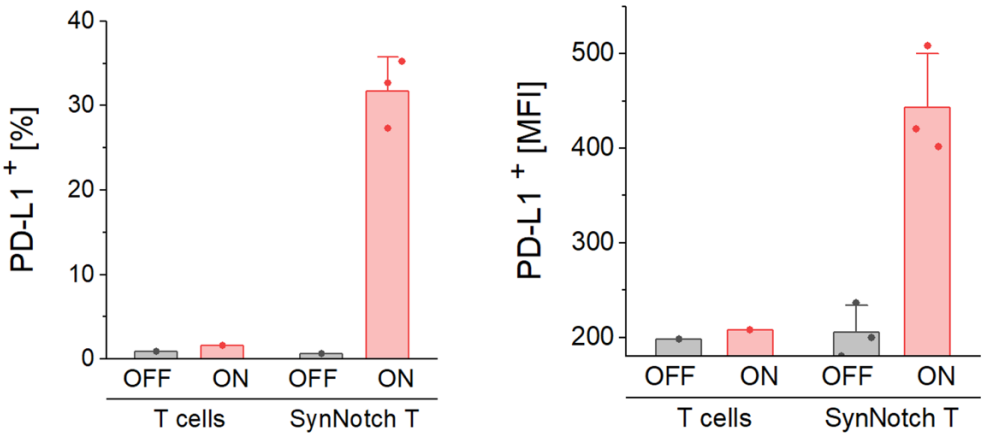

Figure 2. 10: Quantification of PD-L1 expression in synNotch T cells by flow cytometry through percentage of PD-L1$^+$ cells and Median Fluorescence Intensity (MFI) following synNotch activation via plate bound mCherry. Flow cytometry analysis was conducted on cells collected 72 hours after seeding for synNotch activation. SynNotch T cells were stained for expression of synNotch receptors, the expression of constitutive transgene receptors, and the inducible expression of PD-L1. The left panel shows results for the percentage of PD-L1$^+$ cells upon synNotch activation. Parental Jurkat cells display minimal PD-L1 expression, with approximately 0% of cells co-expressing both PD-L1 and the constitutive transgene receptor marker, regardless of whether they are exposed to the activation signal of plate-bound mCherry. Besides, synNotch T cells show around 0% co-expression of PD-L1

and the constitutive transgene receptor in the absence of the activation signal. However, upon exposure to the activation signal, the percentage of double-positive cells for PD-L1 and the constitutive transgene receptor rises significantly to around 32%. The results for median fluorescence intensity (MFI) of PD-L1^{+} cells shows a comparable trend in the right panel. Parental Jurkat cells exhibit minimal PD-L1 expression, with MFI values around 200 for cells with or without the activation signal, respectively. Moreover, synNotch T cells display an MFI value of approximately 200 for PD-L1 expression in the absence of the activation signal. When exposed to the activation signal, the MFI for PD-L1 expression in synNotch T cells increases dramatically to around 450.

It is noted that synNotch activation in fibroblasts is higher than in T cells, which may be due to the greater cell surface contact area of the fibroblasts with the mCherry-bound surface. Overall, the results demonstrate the successful integration and activation of the synNotch circuit in both fibroblasts and T cells with plate bound mCherry. Since PD-L1 expression on the synthetic cells is another crucial criterion for evaluating synNotch activation, the increased surface expression of PD-L1 on the synthetic cells after synNotch activation demonstrates effective integration of the synNotch receptor and activation of the synNotch receptor by plate bound mCherry. Thus, the results of IL-10 secretion and PD-L1 expression in the synthetic cells demonstrate the successful integration and activation of the synNotch circuit by plate-bound mCherry. This establishes the effectiveness of surface-bound mCherry as an activation signal and supports further testing of surfaces to which mCherry can bind for synNotch activation.

2.3 Materials and Methods

2.3.1 Genetic constructs design

The construction of the plasmid was described previously[18]. Briefly, mCherry-responsive synNotch construction: pHR_EF1a_flag- LaM4_synNotch_Gal4-VP64, built from pHR_EF1a_flag-LaM4_synNotch_TetRVP64 (Addgene plasmid#162237) and HR_pGK_LaG17_synNotch_Gal4VP64 (Addgene plasmid# 79127). The response-element plasmid pHR_Gal4UAS_humanIL-

10_T2A_PDL1_PGK_mCherry was purchased[32] (Addgene plasmid#85430). All constructs were cloned via In-Fusion HD Cloning (Takara Bio, 102518).

2.3.2 Lentivirus production

The production of lentivirus was described previously[18]. Briefly, lentivirus production was carried out by co-transfecting pHR cloned plasmids along with vectors encoding the packaging proteins (psPAX2 and pMD2.G) into 70–80% confluent HEK-293T cells seeded in 6-well plates, using Lipofectamine LTX (Thermo Fisher). Viral supernatants were harvested 2–3 days post-transfection, then sterile filtered through a 0.45 μm PES membrane (Genesee Scientific). The viral supernatants were either used directly or concentrated 10× using the LentiX Concentrator (Takara Bio), following the manufacturer's instructions, before being added to cell lines.

2.3.3 Cell culture

NIH/3T3 (ATCC# CRL-1658) were cultured in DMEM (Thermo Fisher) supplemented with 10% Fetal Bovine Serum (Thermo Fisher) and 100 U/mL penicillin/streptomycin (Thermo Fisher). Jurkat, clone E6-1 (ATCC# TIB-152) were culture in standard RPMI 1640 (Gibco) supplemented with 10% heat-inactivated FBS (Gibco), 100 U/mL penicillin/streptomycin (Thermo Fisher), 1 mM sodium pyruvate (Corning), 2 mM L-glutamine (Corning), 10 mM HEPES buffer (Corning) and 50 μM 2-mercaptoethanol (Gibco). Cultures were maintained in a 37 °C incubator with 5% CO_2 and relative humidity (VWR).

2.3.4 Cell line engineering

Cell line engineering was described previously[18]. Briefly, in terms of viral transduction, 20–50 μL concentrated (or equivalent non-concentrated) viral supernatant(s) were added to 5–10 × 10^4 suspended cells in the presense of 10 μg/mL polybrene (Sigma), then transferred into a 12-well plate for 2–3 days before changing to fresh media. Following transduction, all applicable cell lines were selected to ensure

transgene. Cells were sorted for the coexpression of each component using fluorescence-activated cell sorting (FACS) on a FACS ARIA II (Beckton-Dickinson), either by staining with appropriate fluorescently tagged anti-Flag for 30 min at 4 °C (Cell Signaling Technologies), or by detecting transgene expression. A bulk-sorted polyclonal population of engineered cells was used for experiments.

2.3.5 mCherry production

mCherry production was described previously[18]. Briefly, mCherry was purified as an N-terminal hexahistidine fusion protein. For mCherry expression, BL21-AI E.coli (Thermo Fisher) were transformed with mCherry-pBAD (gift from Michael Davidson & Nathan Shaner & Roger Tsien, Addgene plasmid # 54630), grown to an optical density of 0.6 from an overnight-grown glycerol stock, induced with 0.04% w/v L-Arabinose (Sigma), and allowed to express for 5 h. mCherry was purified by NEBExpress Ni Spin Columns (New England Biolabs) according to the manufacturer's instructions, dialyzed against 1× PBS overnight at 4 °C, sterile filtered, and stored at −80 °C for later use.

2.3.6 In vitro stimulation of SynNotch fibroblasts and T cells by plate-bound mCherry

Modified from the previous literature[18], mCherry protein was prepared at a concentration of 70 μg/mL in sterile PBS and added to the well plate at 10 μg/cm². The plate was allowed to dry overnight in a biosafety cabinet, shielded from light, and then washed once with PBS before cell seeding. Anti-mCherry synNotch fibroblasts were seeded at a density of 5×10^4 cells/cm² and cultured for 72 hours after seeding. In contrast, anti-mCherry SynNotch fibroblasts were seeded at a density of 100,000 cells/well in a 96 well plate and cultured for 72 hours after seeding. Following this step, the conditioned medium and the cells were collected for further analysis.

2.3.7 Staining for SynNotch activation and flow cytometry

For synNotch fibroblasts: after SynNotch activation, the anti-mCherry synNotch fibroblasts were detached using TrypLE (Thermo Fisher) and washed once with PBS + 5%FBS. The fibroblasts were then stained for 30min at 4 °C for surface anti-FLAG antibody (Alexa Fluor® 488 Conjugate) (Cell Signaling Technologies) and for surface PD-L1 with anti-PD-L1 BV421 (Biolegend). Cells were then washed twice with PBS + 5%FBS and filtered through 35 μm cell strainer before analysis with Invitrogen™ Attune™ NxT Flow Cytometer.

For synNotch T cells: after SynNotch activation, the anti-mCherry synNotch T cells were pelleted by centrifugation (Thermo Fisher) at 500xg for 5mins and washed once with PBS containing 5% FBS. The T cells were then stained at 4°C for 30 minutes with an Alexa Fluor® 488-conjugated anti-FLAG antibody (Cell Signaling Technologies) and anti-PD-L1 BV421 (BioLegend) for surface PD-L1 expression. Following staining, the cells were washed twice with PBS + 5% FBS and passed through a 35 μm cell strainer before analysis using the Invitrogen™ Attune™ NxT Flow Cytometer.

2.3.8 Enzyme-linked Immunosorbent Assay (ELISA) for quantitative detection of human IL-10

The conditioned medium of SynNotch activation was harvasted for IL-10 ELISA anlysis (Invitrogen). According to the manufacturer's instructions, samples were diluted 1:2 by mixing 50 μL of the sample with 50 μL of Assay Buffer (1x). First, the required number of microwell strips was determined, and the strips were washed twice with Wash Buffer. For standard dilutions, 100 μL of Assay Buffer (1x) was added to the standard wells in duplicate. Then, 100 μL of the prepared standard was added to the first wells, and serial dilutions were created by transferring 100 μL from well to well, discarding 100 μL from the last wells. Alternatively, external standard dilutions could be prepared in tubes and 100 μL of each standard dilution pipetted into the microwell strips. For the blank wells, 100 μL of Assay Buffer (1x) was added, while 50 μL of Assay Buffer (1x) was added to the sample wells, followed by 50 μL of each sample. The Biotin-Conjugate was prepared and 50 μL was added to all wells. The strips were covered and incubated for 2 hours at room temperature (18–25°C). After incubation, Streptavidin-HRP was

prepared, and the microwell strips were emptied and washed three times with Wash Buffer. Then, 100 µL of diluted Streptavidin-HRP was added to all wells. The strips were covered and incubated for 1 hour at room temperature (18–25°C), followed by washing the microwell strips three times with Wash Buffer. Next, 100 µL of TMB Substrate Solution was added to all wells, and the microwell strips were incubated for approximately 10 minutes at room temperature (18–25°C). Following incubation, 100 µL of Stop Solution was added to each well. Finally, the color intensity was measured at 450 nm by a plate reader (BioTek).

References

1. Hubbell, J. A. (2024). Immunoengineering a Future of Molecular, Material, and Cellular Therapeutics. *The Journal of Immunology*, *212*(2), 167-168.
2. Backlund, C., Jalili-Firoozinezhad, S., Kim, B., & Irvine, D. J. (2023). Biomaterials-mediated engineering of the immune system. *Annual review of immunology*, *41*(1), 153-179.
3. Yousefpour, P., Ni, K., & Irvine, D. J. (2023). Targeted modulation of immune cells and tissues using engineered biomaterials. *Nature reviews bioengineering*, *1*(2), 107-124.
4. Hosseinalizadeh, H., Rabiee, F., Eghbalifard, N., Rajabi, H., Klionsky, D. J., & Rezaee, A. (2023). Regulating the regulatory T cells as cell therapies in autoimmunity and cancer. *Frontiers in Medicine*, *10*, 1244298.

Chapter 3: SynNotch activation by biomaterials

3.1 Introduction

Biomaterials have emerged as powerful tools in regenerative medicine and immunoengineering, offering the ability to modulate the immune response in the field of regeneration[1]. By incorporating engineered cells with synthetic receptors, such as synNotch, biomaterials can be tailored to create highly programmable systems for therapeutic applications. Hyaluronic acid (HA) gel and poly(lactic-co-glycolic acid) (PLGA) particles are widely used biomaterials in regenerative medicine and drug delivery, offering significant advantages for clinical applications[2,3]. HA gel, a naturally occurring and highly biocompatible substance, provides a hydrated environment that supports cell viability and promotes tissue repair[2]. It is easily modified for injectable use, making it ideal for localized therapies[2]. PLGA particles, on the other hand, are biodegradable and FDA-approved, with a tunable degradation rate, allowing for controlled, sustained release of therapeutic agents[3]. Both materials are safe, versatile, and suitable for minimally invasive procedures, making them strong candidates for use in synNotch receptor-based therapies, where they enable controlled activation of engineered cells for targeted immune modulation and tissue regeneration[2,3]. In this chapter, the incoporation of biomaterials into synNotch circuit is investigated.

3.2 Results and Discussion

3.2.1 SynNotch activation by mCherry conjugated to microparticle

To test and manipulate the surfaces to which mCherry can bind, mCherry was conjugated to microparticles (i.e., PLGA particles) using EDC/NHS chemistry. The schematic of synNotch activation by PLGA particles is shown **(Figure 3.1)**. When bound to PLGA particles, mCherry serves as an activation signal to activate the synNotch fibroblasts.

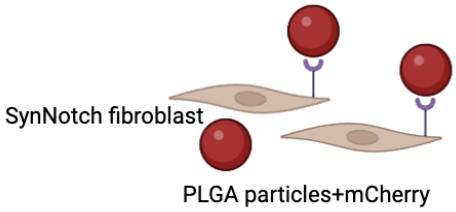

Figure 3. 11: Schematic representation of the synNotch activation by PLGA particles. mCherry was conjugated to PLGA particles using EDC/NHS chemistry. When bound to PLGA particles, mCherry can act as an activation signal to activate the synNotch fibroblasts. Activation of synNotch fibroblasts were further evaluated through flow cytometry analysis.

The mCherry conjugated PLGA particles were first imaged using a microscope to confirm the successful conjugation of mCherry to the PLGA particles **(Figure 3.2)**. As shown in the figure, mCherry-conjugated PLGA particles exhibit a distinct mCherry fluorescence signal compared to non-conjugated (plain) PLGA particles. The overlay image confirms that the fluorescence signal is attributable to the mCherry-conjugated PLGA particles, not due to false positive background.

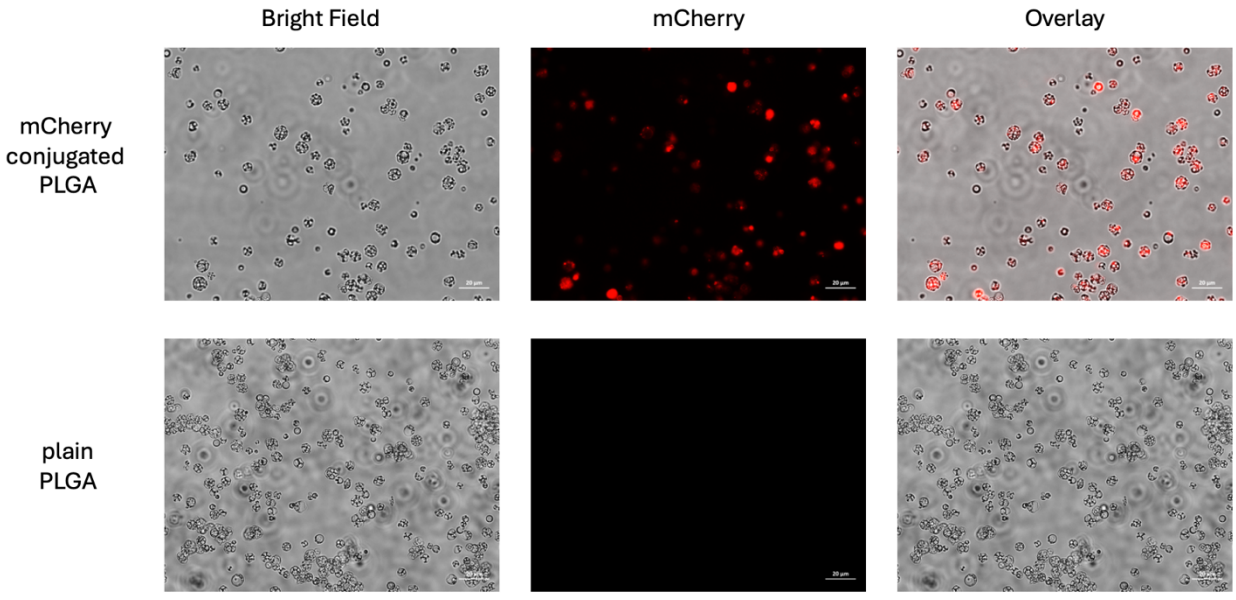

Figure 3. 12: Fluorescence microscopy images of non-conjugated (plain) and mCherry-conjugated PLGA particles. The signal of mCherry fluorscence was detected using a microscope. mCherry-conjugated PLGA particles

produce a clear mCherry fluorescence signal, whereas the plain PLGA particles do not. The overlay image verifies that this fluorescence signal originates from the mCherry-conjugated PLGA particles and is not a result of false positive background.

The size of the mCherry conjugated PLGA particle is also characterized and compared to the plain PLGA particle **(Figure 3.3)**. As shown in the figure, there is no significant difference between the plain and mCherry-conjugated particles, with both exhibiting a size of approximately 6 micrometers.

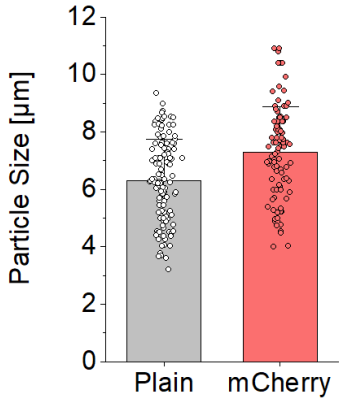

Figure 3. 13: Size characterization of plain and mCherry conjugated PLGA particles. There is no significant difference in size between the plain and mCherry-conjugated particles, with both measuring approximately 6 micrometers.

SynNotch activation was then assessed in the cells after co-incubation of mCherry-conjugated PLGA particles with synNotch fibroblasts. Anti-mCherry synNotch fibroblasts were seeded at a density of 5×10^4 cells/cm² and cultured for 72 hours for synNotch activation. Non-conjugated or mCherry conjugated PLGA particles were added to the cells at a ratio of 10 particles per cell. Afterward, the cells were collected, and flow cytometry analysis was conducted to assess synNotch activation via mCherry conjugated PLGA particles. Upon collection, synNotch fibroblasts were stained for synNotch receptor, consitutive transgene receptor marker, and the induciable expression of PD-L1 for synNotch activation. A representive dot plot for flow cytometry for synNotch activation via mCherry conjugated PLGA particle is shown for synNotch fibroblast **(Figure 3.4)**. In this figure, after co-incubation with the activation signal

of mCherry-conjugated PLGA particles, synNotch fibroblasts show a 36.4% PD-L1^{+} population, demonstrating a significant increase compared to synNotch fibroblasts co-incubated with plain PLGA particles in the absence of the activation signal.

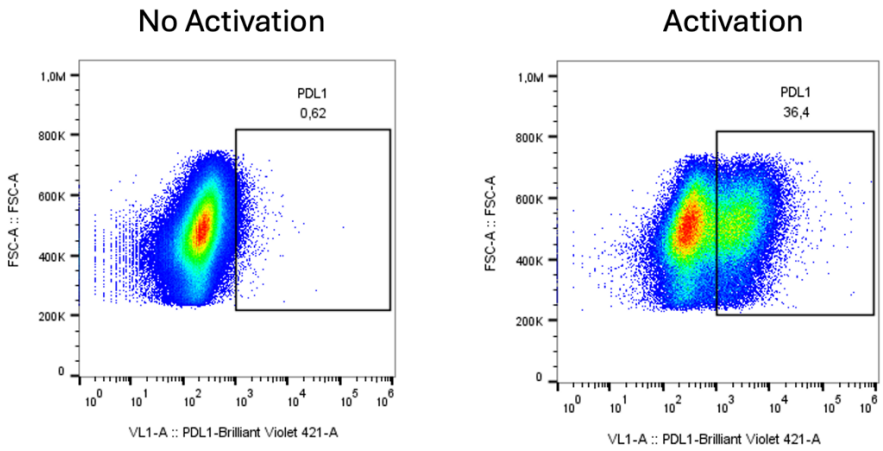

Figure 3. 14: Representive dot plot for flow cytometry for synNotch fibroblasts upon synNotch activation via mCherry conjugated PLGA particles. Flow cytometry analysis was conducted on cells collected 72 hours after seeding for synNotch activation. SynNotch fibroblasts were stained for expression of synNotch receptors, the expression of constitutive transgene receptors, and the inducible expression of PD-L1. After co-incubation with the activation signal from mCherry-conjugated PLGA particles, synNotch fibroblasts exhibit a 36.4% PD-L1+ population, reflecting a significant increase compared to synNotch fibroblasts co-incubated with plain PLGA particles without the activation signal.

Thus, the results of PD-L1 expression on the synthetic cells demonstrate the successful activation of the synNotch receptor by mCherry conjugated PLGA particles. By manipulating the surfaces to which mCherry can bind, mCherry-conjugated PLGA particles enhance the flexibility of creating a local immunosuppressive environment. They offer a viable option for SynNotch activation in the local setting. Due to the relatively slow degradation of the PLGA particles, mCherry-conjugated particles provide sustained SynNotch activation, enabling prolonged release of IL-10 and extended immunosuppressive function.

3.2.2 SynNotch activation by mCherry conjugated to HA gel

To explore alternative options for local SynNotch activation, mCherry was bound to a different surface, specifically the HA gel. The HA gel was created through the crosslinking reaction of HA and BDDE, and mCherry was subsequently conjugated to the crosslinked HA gel through EDC/NHS chemistry. The schematic of synNotch activation by HA gel is shown **(Figure 3.5)**. When bound to HA gel, mCherry serves as an activation signal to activate the synNotch fibroblasts and T cells.

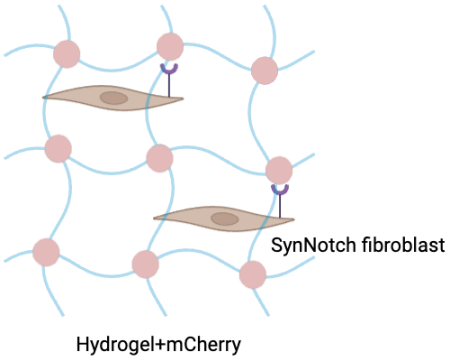

Figure 3. 15: Schematic representation of the synNotch activation by HA gel. The HA gel was generated through the crosslinking reaction of HA and BDDE, and mCherry was conjugated to HA gel via EDC/NHS chemistry. When conjugated to the HA gel, mCherry can act as an activation signal to activate the synNotch fibroblasts and T cells. Activation of synNotch fibroblasts and T cells were further evaluated through flow cytometry analysis.

The mCherry conjugated HA gel was first imaged using a microscope to confirm the successful conjugation of mCherry to the HA gel. mCherry-conjugated HA gel shows a distinct mCherry fluorescence signal compared to non-conjugated HA gel. To test synNotch activation by the mCherry-conjugated HA gel, anti-mCherry SynNotch fibroblasts or T cells were seeded on the gel and co-incubated with it for 72 hours. Afterward, the cells were collected and synNotch activation was assessed via flow cytometry analysis. Upon collection, synNotch fibroblasts or T cells were stained for synNotch receptor, consitutive transgene receptor marker, and the induciable expression of PD-L1 for synNotch activation. Representive dot plots for flow cytometry for synNotch activation via mCherry conjugated HA gel is shown for synNotch fibroblasts and T cells **(Figure 3.6)**. In this figure, after co-incubation with the

activation signal of mCherry-conjugated HA gel, synNotch fibroblasts show a 94.6% PD-L1^{+} population, demonstrating a significant increase compared to their unstained control, which was not exposed to the activation signal **(Figure 3.6, left)**. Similarly, after co-incubation with the activation signal of mCherry-conjugated HA gel, synNotch T cells exhibit a 74.0% PD-L1^{+} population, showing a significant increase compared to their unstained control, which was not exposed to the activation signal **(Figure 3.6, left)**.

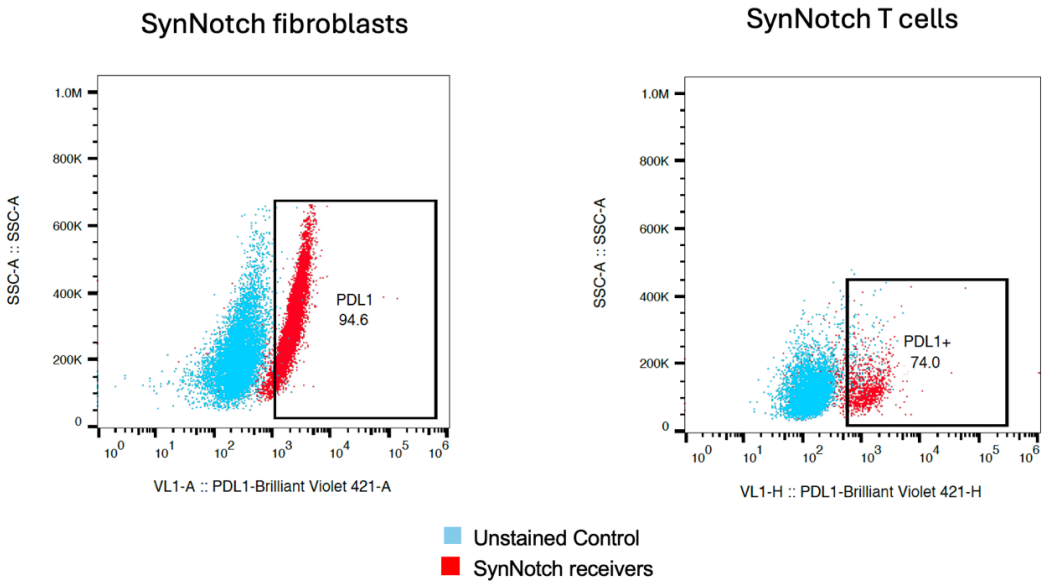

Figure 3. 16: Representive dot plots for flow cytometry for synNotch fibroblasts and T cells upon synNotch activation via mCherry conjugated HA gel. Flow cytometry analysis was conducted on cells collected 72 hours after seeding for synNotch activation. SynNotch fibroblasts or T cells were stained for expression of synNotch receptors, the expression of constitutive transgene receptors, and the inducible expression of PD-L1. The blue colored dots represent individual cells from the sample of the corresponding unstained control while the red colored dots represent individual cells from the sample of the anti-mCherry synNotch receptor cells (i.e., synNotch receivers). In the left panel, after co-incubation with the activation signal of mCherry-conjugated HA gel, synNotch fibroblasts display a 94.6% PD-L1^{+} population, indicating a significant increase compared to the unstained control, which was not exposed to the activation signal. In the right panel, similarly, synNotch T cells, following co-incubation with the activation signal of the mCherry-conjugated HA gel, show a 74.0% PD-L1^{+} population, demonstrating a significant increase compared to their unstained control, which did not receive the activation signal.

The results of PD-L1 expression on the synthetic cells illustrate the successful activation of the synNotch receptor by mCherry-conjugated HA gel. This approach offers an additional method for manipulating surfaces to which mCherry can bind, expanding the flexibility in creating a local immunosuppressive environment. Given the high biocompatibility of HA gel and its extensive use in clinical research, the mCherry-conjugated HA gel enhances the potential of the synthetic system for use in clinical studies, making it a promising immunotherapeutic approach for regenerative medicine.

3.3 Materials and Methods

3.3.1 Microparticle preparation, conjugation, and characterization

Modified from the method which was described previously[33], poly(lactic-co-glycolic acid) (PLGA) particles were prepared by dissolving poly(D,L-lactic-co-glycolide) (Polysciences) in dichloromethane (DCM) (Sigma) to create a 25 mg/mL PLGA solution. 5 mL of the prepared PLGA solution was then added dropwise to 45 mL of 1% polyvinyl alcohol (PVA) solution (Sigma). The mixture was homogenized using a homogenizer (IKA) at 10,000 rpm for 10 minutes. After homogenization, the entire volume (50 mL) was transferred to 450 mL of 0.1% PVA solution, and the suspension was stirred at room temperature for at least 6 hours to allow for solvent evaporation. The particles were then collected via centrifugation (Thermo Fisher) at 500 × g for 5 minutes and washed three times with distilled water. Based on the method described previously[18], PLGA particles were treated with a 250 mM solution of 1-Ethyl-3-(3-dimethylaminopropyl)carbodiimide (EDC, Sigma) and N-Hydroxysuccinimide (NHS, Sigma), followed by two washes with phosphate-buffered saline (PBS, pH 7.4). The particles were then incubated overnight at 4°C with inversion mixing in a concentration of mCherry of 300 µg/mL in PBS. Solution changes during the washing steps were accomplished through centrifugation (Thermo Fisher) at 500 × g for 5 minutes. The particle size and concentration were determined using a Zeiss Axio Observer Z1 and a hemocytometer (Sigma). The resulting particles were stored at -80°C until further use.

3.3.2 In vitro stimulation of SynNotch fibroblasts by microparticles

PLGA particles, either plain or conjugated with mCherry, were added to the wells at a ratio of 10 particles per cell during the seeding of anti-mCherry synNotch fibroblasts. The cells were seeded at a density of 50,000 cells/cm². For synNotch activation, the anti-mCherry synNotch fibroblasts were incubated for 72 hours after seeding. Following this step, the cells were detached for further analysis.

3.3.3 Hydrogel preparation, conjugation, and characterization

Hyaluronic acid (HA) (200-400 kDa, 2% w/v, Bloomage Biotechnology) was dissolved in 0.25 M NaOH. 1,4-Butanediol diglycidyl ether (BDDE, Sigma) was then added to the HA solution to achieve a final concentration of 14% (w/v). The reaction was carried out at 40 °C for a minimum of 6 hours. Afterward, the reaction mixture was thoroughly washed with PBS at least three times to obtain the final hydrogel product. The mCherry protein was conjugated to the HA gel using EDC/NHS chemistry. Prior to activation, the HA gel was thoroughly washed with PBS, and the pH of the wash was confirmed to be approximately 7.4. EDC (20 mg) was dissolved in 5 mL of sterile water and filtered for sterilization. The EDC solution was added dropwise to the HA gel, which was then placed on a shaker for 15 minutes to initiate the reaction. NHS (20 mg) was dissolved in 1 mL of PBS, sterile-filtered, and 20 µL of this solution was added per 1 mL of EDC solution. The reaction was allowed to proceed for 40 minutes. The mCherry protein was then added to achieve a final concentration of 135.5 µg/mL in PBS for a 0.5 mL gel volume. The reaction mixture was incubated overnight at 4°C. After overnight incubation, the HA gel conjugated with mCherry protein was imaged using Zeiss Axio Observer Z1 to confirm the success of the conjugation.

3.3.4 In vitro stimulation of SynNotch fibroblasts and T cells by hydrogel

2 million synNotch fibroblasts or T cells were seeded on top of the HA gel conjugated with the mCherry. For synNotch activation, the anti-mCherry synNotch fibroblasts or T cells were incubated for 72 hours after seeding. Following this step, the cells were collected for further analysis.

References

1. Sadtler, K., Singh, A., Wolf, M. T., Wang, X., Pardoll, D. M., & Elisseeff, J. H. (2016). Design, clinical translation and immunological response of biomaterials in regenerative medicine. *Nature Reviews Materials*, *1*(7), 1-17.
2. Gentile, P., Chiono, V., Carmagnola, I., & Hatton, P. V. (2014). An overview of poly (lactic-co-glycolic) acid (PLGA)-based biomaterials for bone tissue engineering. *International journal of molecular sciences*, *15*(3), 3640-3659.
3. Horvath, D., & Basler, M. (2023). PLGA particles in immunotherapy. *Pharmaceutics*, *15*(2), 615.

Chapter 3: Functionality of synthetic cells

3.1 Introduction

The synNotch receptor system offers a powerful tool for engineering cells with precise control over immune responses, particularly for immunosuppressive functions. By designing synthetic cells that express immunoregulatory molecules such as IL-10 and PD-L1 upon activation, the synNotch system can be harnessed to create localized immunosuppressive environments[1]. These engineered cells respond to specific external signals, such as surface-bound mCherry, to modulate immune activity in a highly localized and prelonged manner. This approach holds great potential for applications in autoimmune diseases, transplantation, and regeneration, where controlling immune responses is critical. By activating synNotch receptors in response to specific cues, these synthetic cells can help mitigate immune rejection and support long-term graft survival, offering a novel immunoengineering strategy for clinical use. Since IL-10 and PD-L1 function through distinct pathways[2], their combination in the designed circuit can achieve a synergistic dual effect in immunosuppression.

3.2 Results and Discussion

3.2.1 Conditioned medium from synNotch activation promotes Treg formation in vitro

To evaluate the immunosuppressive function of synNotch activation in synthetic cells, mouse primary $CD4^+$ T cells were co-incubated with the conditioned medium from synNotch activation to assess the formation of Tregs in vitro. After seeding with plate bound mCherry for 72hrs, the conditioned medium of synNotch fibroblasts from synNotch activation was collected and co-incubated with mouse primary $CD4^+$ T cells. Mouse primary $CD4^+$ T cells were isolated by negative selection from C.Cg-*Foxp3*^{tm2Tch}/J mice and then activated. For T cell activation, wells were coated with anti-mouse CD3 antibody at 10 µg/mL for 2.5–3 hours at 37°C prior to seeding. Human IL-2 (25,000 U/mL), soluble anti-mouse CD28 (2 µg/mL) antibody and TGF-β (5ng/mL) were also added to the cell culture for T cell activation and Treg formation. Five days after co-incubation, cells were harvested and assessed via flow cytometry analysis.

A representive dot plot for flow cytometry for Treg formation after co-incubation with conditioned medium from synNotch activation in vitro is shown **(Figure 3.17)**. In this figure, the conditioned medium from SynNotch activation, when supplemented with TGF-β, generates a 31.8% FOXP3^{+} population, indicating an increased formation of Tregs compared to the sample with conditioned medium that had no synNotch activation when supplemented with TGF-β, which generates only 15.7% FOXP3^{+} cells. In contrast, the conditioned medium without synNotch activation and without the addition of TGF-β results in a low percentage of Treg population, with only 3.78% FOXP3^{+} cells.

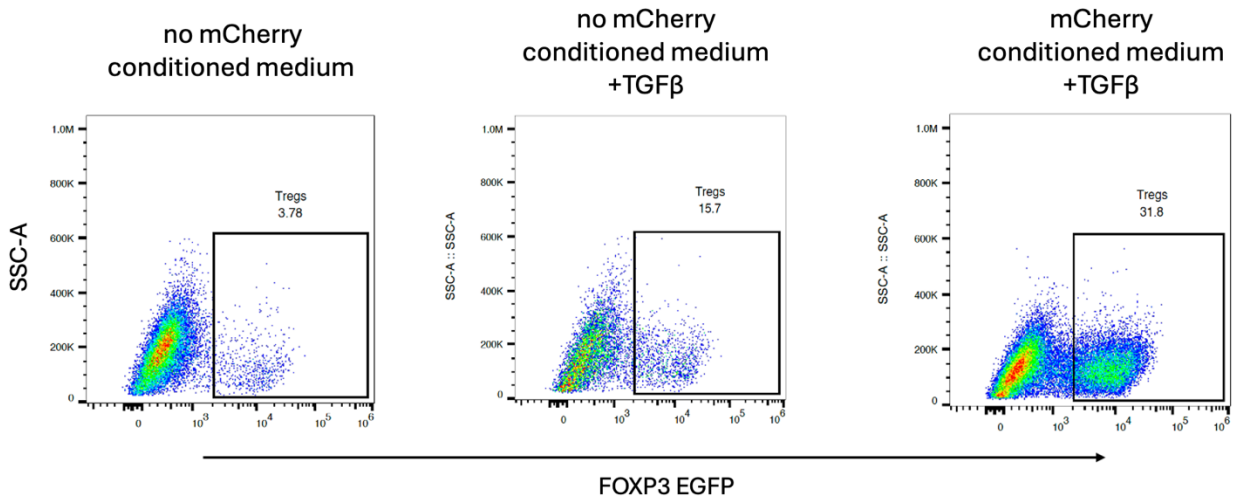

Figure 3. 17: A representive dot plot for flow cytometry for Treg formation after co-incubation with conditioned medium from synNotch activation in vitro. After seeding with plate-bound mCherry for 72 hours, the conditioned medium from synNotch fibroblasts following synNotch activation was collected and co-incubated with mouse primary CD4^{+} T cells. The mouse primary CD4^{+} T cells were isolated from C.Cg-Foxp3^{tm2Tch}/J mice using negative selection and subsequently activated. For T cell activation and Treg formation, wells were coated with anti-mouse CD3 antibody (10 µg/mL) and human IL-2 (25,000 U/mL), soluble anti-mouse CD28 antibody (2 µg/mL), and TGF-β (5 ng/mL) were added to the culture. Five days post co-incubation, the cells were harvested and analyzed by flow cytometry. The conditioned medium from SynNotch activation, when supplemented with TGF-β, results in a 31.8% FOXP3^{+} population, indicating increased Treg formation compared to the conditioned medium from cells without SynNotch activation, which yields only 15.7% FOXP3^{+} cells when supplemented with TGF-β. In

contrast, the conditioned medium without SynNotch activation and without TGF-β results in a low percentage of Treg population, with only 3.78% FOXP3$^+$ cells.

Thus, the FOXP3$^+$ cell population results demonstrate the successful formation of Tregs in vitro following synNotch activation, indicating the establishment of a local immunosuppressive environment and highlighting the immunosuppressive function of the synthetic cells. This in vitro achievement of synNotch activation suggests strong potential for advancing this system to in vivo experiments and clinical studies.

3.3 Materials and Methods

3.3.1 Mouse primary CD4$^+$ T cells isolation, in vitro Treg formation, staining and flow cytometry

Mouse primary CD4$^+$ T cells were isolated by negative selection (STEMCELL Technologies) from C.Cg-*Foxp3*^{tm2Tch}/J mice (The Jackson Laboratory) and then activated. For T cell activation, wells were coated with anti-mouse CD3 antibody (Bio X Cell) at 10 μg/mL for 2.5–3 hours at 37°C. After spleen isolation, the tissue was processed through a 40 μm cell strainer in PBS+2% HI-FBS on ice, followed by centrifugation at 500×g for 5 minutes. The cells were then treated with ACK Lysing Buffer (Gibco), followed by centrifugation at 500×g for 5 minutes. According to the manufacturer's instructions, cells were resuspended in PBS without Ca^{2+} or Mg^{2+}, containing 1 mM EDTA. The cell suspension was incubated with rat serum and magnetic beads, followed by magnetic separation. Cells were resuspended, counted, and seeded at a density of 300,000 cells/well in a 96-well plate. Human IL-2 (25,000 U/mL, PeproTech), soluble anti-mouse CD28 (2 μg/mL, Bio X Cell) antibody and TGF-β (5ng/mL, PeproTech) were added to the cell culture. After 5 days of incubation at 37°C, mouse primay CD4$^+$ T cells were collected and stained for flow cytometry analysis.

References

1. Lamichhane, P., Karyampudi, L., Shreeder, B., Krempski, J., Bahr, D., Daum, J., ... & Knutson, K. L. (2017). IL10 release upon PD-1 blockade sustains immunosuppression in ovarian cancer. *Cancer research*, *77*(23), 6667-6678.
2. Brooks, D. G., Ha, S. J., Elsaesser, H., Sharpe, A. H., Freeman, G. J., & Oldstone, M. B. (2008). IL-10 and PD-L1 operate through distinct pathways to suppress T-cell activity during persistent viral infection. *Proceedings of the National Academy of Sciences*, *105*(51), 20428-20433.

Chapter 4: Future Directions

Through this thesis, we have successfully demonstrated the generation and application of a SynNotch system with immunosuppressive capabilities, highlighting its potential for treating autoimmune diseases such as Type 1 Diabetes (T1D). Using mCherry as a model activation signal, we showed the flexibility in manipulating this activation signal through its conjugation to PLGA particles and HA gel, which can be implanted into the body for future clinical use. The ability to bind mCherry to different materials offers a versatile approach for synNotch activation, providing a platform for potential therapeutic interventions that could be tailored for specific clinical scenarios.

In addition to demonstrating the flexibility of the activation signal, we validated the functionality of our synthetic circuit in terms of creating an immunosuppressive environment. This was achieved by activating synNotch in fibroblasts and T cells, resulting in the secretion of immunosuppressive factors such as IL-10 and the expression of PD-L1 on the surface of the synthetic cells. These results lay a strong foundation for further development and testing, especially regarding the translation of this system into in vivo models and clinical studies.

Through this approach, we also established that the synNotch circuit can be successfully integrated into synthetic cells, demonstrating its versatility across different cell types. While fibroblasts and T cells were the primary focus of our experiments, the potential for synNotch integration in other cell types opens new possibilities for broader applications in cell engineering and immunotherapy. The successful integration of the synNotch circuit into both fibroblasts and T cells with plate-bound mCherry activation signals underscores the system's adaptability and effectiveness in creating a controlled immunosuppressive environment.

A critical aspect of our designed circuit for synNotch activation is the secretion of IL-10, a key immunosuppressive cytokine. The increased IL-10 secretion observed in the conditioned medium following synNotch activation confirms the successful integration and function of the synNotch receptor, providing a clear indicator of the system's immunosuppressive potential. Additionally, the expression of

PD-L1, another marker of immune regulation, further validates the system's functionality. The enhanced PD-L1 surface expression after SynNotch activation serves as a crucial measure of the synthetic cells' ability to mediate local immune suppression, supporting the system's therapeutic potential.

Moreover, by incorporating mCherry-conjugated PLGA particles as the activation surface, we demonstrated that the SynNotch system can be activated in a localized and sustained manner. The slow degradation rate of PLGA particles provides prolonged synNotch activation, resulting in extended release of IL-10 and sustained immunosuppressive effects. This prolonged activation adds a valuable dimension to the therapeutic potential of synNotch, allowing for more durable immune regulation in clinical applications.

In a parallel approach, we explored the use of mCherry-conjugated HA gel as an activation surface. The high biocompatibility of HA gel, combined with its widespread use in clinical research, makes it an attractive option for localized SynNotch activation. The successful activation of SynNotch via mCherry-conjugated HA gel further expands the flexibility of the system in creating an immunosuppressive environment. This opens promising avenues for using the SynNotch system in clinical studies, particularly in regenerative medicine, where localized immune modulation can enhance protection and reduce immune-mediated rejection.

Additionally, the results of $FOXP3^+$ Treg formation following SynNotch activation further demonstrate the system's immunosuppressive capacity. The increase in Treg population upon co-incubation with the conditioned medium from synNotch-activated cells highlights the system's ability to modulate the immune response effectively. This achievement underscores the potential of the synNotch system to create a controlled immunosuppressive environment in vitro, paving the way for future in vivo experiments and clinical applications aimed at treating autoimmune disorders.

Looking ahead, two mouse models can be developed to evaluate the functionality of our synthetic cell system in vivo. The first one is the ectopic bone formation model in immunocompetent mice. The schematic of this model is shown **(Figure 4.1)**. In this model, human mesenchymal stem cells (hMSCs)

are co-injected subcutaneously with biomaterials and synthetic cells on the back of the mouse. With the knowledge that the osteogenic potential of MSCs is known to be influenced by their interactions with the recipient immune system[1], the goal of this model is to assess whether the synthetic cells can protect the hMSCs in the host environment, allowing them to form bone structures, which will be monitored over time using microCT.

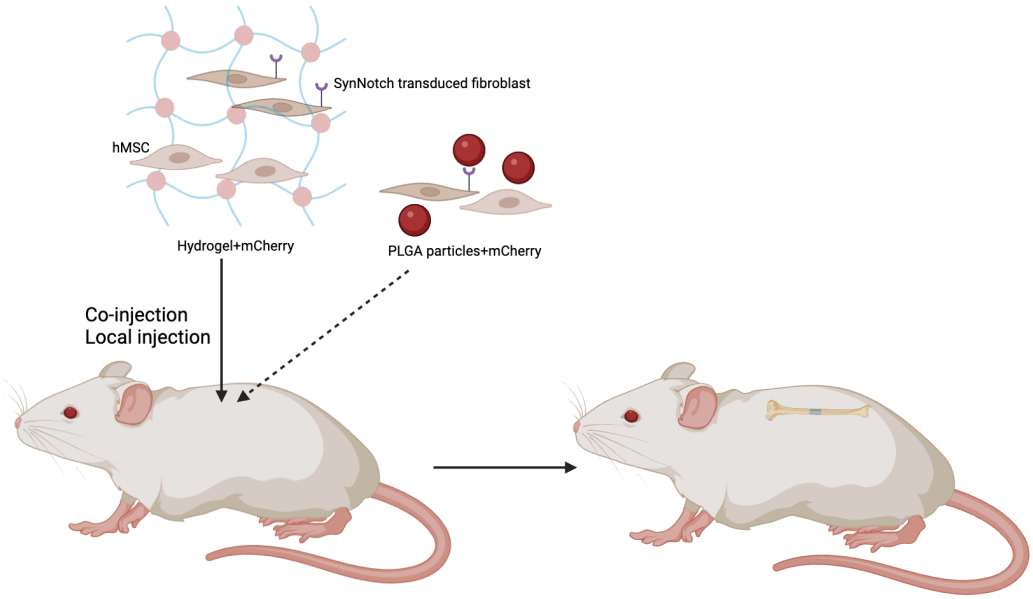

Figure 4. 1: Schematic of the ectopic bone formation model in immunocompetent mice. Human mesenchymal stem cells (hMSCs) are co-injected subcutaneously with biomaterials and synthetic cells on the back of the mouse. The aim of this model is to determine whether the synthetic cells can protect the hMSCs in the host environment, enabling them to form bone structures. Bone formation will be monitored over time using microCT.

Another mouse model is the beta islet transplation model. The schematic of this model is shown **(Figure 4.2)**. In this model, beta islets are isolated from a donor mouse and co-injected with mCherry-bound hydrogel or PLGA particles and synNotch-transduced fibroblasts. The goal is to create an immunosuppressive environment through synNotch activation, protecting the transplanted beta islets from immune attack in a recipient mouse of a different strain. Glucose levels will be monitored over time to assess the success of the transplantation. Both synNotch fibroblasts and T cells are tested in this system:

fibroblasts are co-injected directly with the beta islets, while T cells are administered systemically. This allows T cells to travel and become activated at the specific site of the biomaterial, complementing the localized immunosuppressive effect created by the fibroblasts. These two models will further validate the system's therapeutic potential for creating immunosuppressive environments, moving it closer to clinical application.

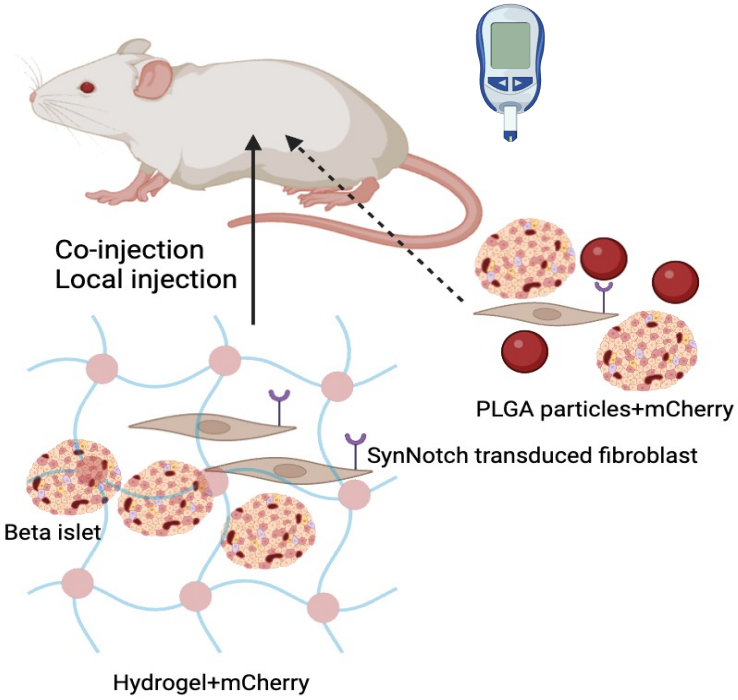

Figure 4. 2: Schematic of the beta islet transplation model. In this model, beta islets are isolated from a donor mouse and co-injected with mCherry-bound hydrogel or PLGA particles along with SynNotch-transduced fibroblasts. The aim is to establish an immunosuppressive environment via SynNotch activation, thereby protecting the transplanted beta islets from immune attack in a recipient mouse of a different strain. Glucose levels will be monitored over time to evaluate the success of the transplantation. The system tests both SynNotch fibroblasts and T cells: fibroblasts are injected directly with the beta islets, while T cells are administered systemically. This approach allows T cells to migrate and activate at the biomaterial site, enhancing the localized immunosuppressive effect generated by the fibroblasts.

In conclusion, the successful development and implementation of the synNotch system with immunosuppressive capabilities offer a novel approach for treating autoimmune diseases and promoting regenerative medicine. The synNotch system we developed offers a highly adaptable platform for creating localized immunosuppressive environments, with demonstrated success in both fibroblasts and T cells. By demonstrating the flexibility of using mCherry bound PLGA particles and HA gel for synNotch activation, we have expanded the potential for localized immune modulation in therapeutic applications. The in vitro results, including enhanced IL-10 secretion, PD-L1 expression, and Treg formation, underscore the effectiveness of this system in establishing an immunosuppressive environment. With future in vivo studies utilizing ectopic bone formation and beta islet transplantation models, we aim to further validate the therapeutic potential of the synNotch system. These findings lay the groundwork for advancing this technology into clinical applications, where it holds promise as a customizable, localized immunotherapeutic strategy for regenerative medicine and autoimmune diseases.

References

1. Hasani-Sadrabadi, M. M., Sarrion, P., Pouraghaei, S., Chau, Y., Ansari, S., Li, S., ... & Moshaverinia, A. (2020). An engineered cell-laden adhesive hydrogel promotes craniofacial bone tissue regeneration in rats. *Science translational medicine*, *12*(534), eaay6853.